



UDC 581.526.325(265.53)“322”

DOI: 10.21072/mbj.2022.07.4.07

PHYTOPLANKTON PRIMARY PRODUCTION ON THE NORTHEASTERN SAKHALIN ISLAND SHELF IN SUMMER

© 2022 P. P. Tishchenko

V. I. Il'ichev Pacific Oceanological Institute FEB RAS, Vladivostok, Russian Federation

E-mail: eq15@poi.dvo.ru

Received by the Editor 19.04.2021; after reviewing 25.10.2021;
accepted for publication 26.09.2022; published online 29.11.2022.

The eastern Sakhalin Island shelf is the area of high biological production. Its key peculiarity is the presence of a feeding area for the Okhotsk–Korean population of gray whales. We aimed at determining the features of the formation of primary production in this area; thereby, on 7–9 July, 2016, hydrochemical studies on the northeastern Sakhalin Island shelf were carried out. At each station, water was sampled from surface and near-bottom layers; then, concentrations of chlorophyll *a*, nitrates, and phosphates were measured. Moreover, at each station, depth profiling was conducted by a Sea-Bird SBE 19plus and a Rinko-Profiler. Those profilers were equipped with sensors for pressure, temperature, electrical conductivity, chlorophyll fluorescence, dissolved oxygen, turbidity, and photosynthetically active radiation. Assimilation number for phytoplankton was measured *in situ* by ARO1-USB Rinko dissolved oxygen sensors (JFE Advantech Co., Ltd.). Phytoplankton primary production in the photic layer was determined by the light model based on the representation of the photosynthetic light-response curve in the modified model of the non-rectangular hyperbola. Most intensively, the primary production occurred in the area affected by the Amur River. In the photic layer, the values of integral primary production varied within 1.57–11.17 g C·m⁻²·day⁻¹. The distribution area of the modified highly productive water of the Amur River reached the traverse of the southern boundary of the Piltun Bay; there, it was limited by cold salty water which had risen due to the eddy structure from deeper horizons. The ratio of the production spent on the food supply formation for the Okhotsk–Korean population of gray whales was 1.9 % of the total production of the studied water area.

Keywords: phytoplankton primary production, Amur River, Sakhalin Island, gray whale

The Sea of Okhotsk is a basin of high biological productivity. Here, the total annual production of organic matter varies within 17.85–23.9 billion tons wet weight, and out of it, 63–78 % is primary production (Shuntov et al., 2019). The Sakhalin Island shelf is one of the main productivity areas of the Sea of Okhotsk. In April–November, the southeastern slope is characterized by monthly mean values of phytoplankton primary production (hereinafter PP) of 0.4–0.6 g C·m⁻²·day⁻¹ (Kasai & Hirakawa, 2015). During the phytoplankton bloom, PP can reach 4–6 g C·m⁻²·day⁻¹ in the Piltun Bay area (Sorokin Yu. & Sorokin P., 1999) and 1.9 g C·m⁻²·day⁻¹ abeam the southern boundary of the Chayvo Bay (Isada et al., 2009). Changes in water productivity on the eastern Sakhalin Island shelf are mostly related to the flow volume of the Amur River (Tskhay et al., 2015).

Moreover, the eastern Sakhalin Island shelf is of great interest since it is a feeding area for the Okhotsk–Korean population of gray whales. In the middle XX century, those were considered exterminated but later gray whales were found off the Sakhalin Island. To date, this population is included in the Red List of the International Union for Conservation of Nature.

Due to the importance of analyzing such a highly productive area of the World Ocean, on 7–9 July, 2016, hydrochemical studies of the northeastern Sakhalin Island shelf were carried out. The investigation was aimed at determining the features of the formation of PP there (Tishchenko et al., 2018).

MATERIAL AND METHODS

The work was carried out during the cruise of the RV “Professor Gagarinsky” in July 2016 (Tishchenko et al., 2018). There were 33 stations on the eastern slope of Sakhalin; their location is shown in Fig. 1. At each station, vertical profiling of the water column was carried out with Sea-Bird SBE 19plus V and Rinko-Profiler; those were equipped with sensors for pressure, temperature, electrical conductivity, chlorophyll fluorescence, dissolved oxygen, turbidity, and photosynthetically active radiation (hereinafter PAR). Moreover, at each station, water was sampled from surface and near-bottom layers with 5-L Niskin bottles, and concentrations of chlorophyll *a* (hereinafter Chl), nitrates, and phosphates were measured. A total of 66 water samples were taken to determine each parameter.

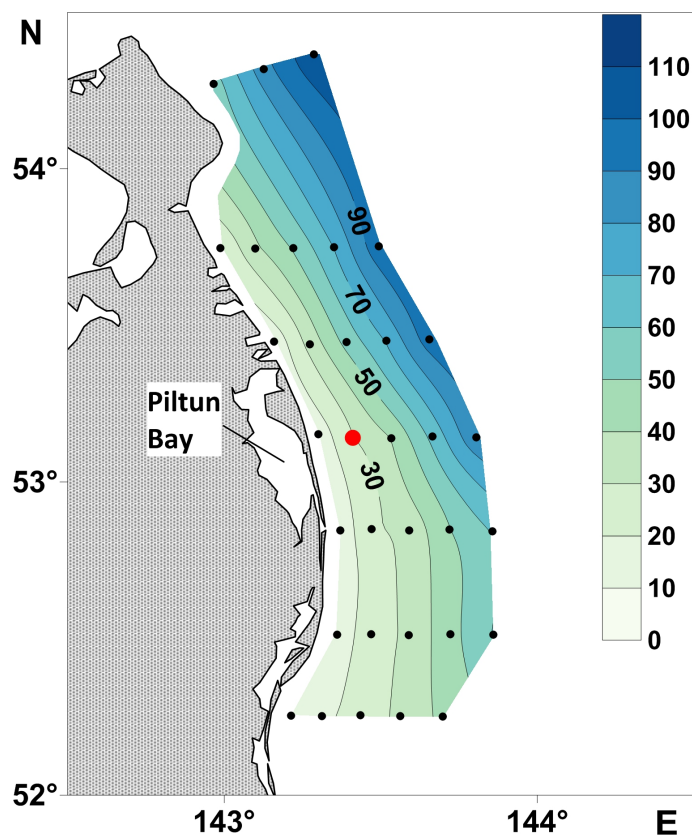


Fig. 1. Map of depth and location of stations during the study on the northeastern Sakhalin Island shelf (71st cruise of the RV “Professor Gagarinsky”, 7–9 July, 2016). The red point denotes the station where the assimilation number for phytoplankton was measured

The nutrients were measured on the day of sampling in the laboratory onboard. Phosphates were determined by the Murphy–Riley method modified by Korolev (ascorbic acid was used as a reducing agent) (Metody gidrokhimicheskikh issledovani, 1988). Nitrates were preliminarily reduced to nitrites in a cadmium reducer and then determined by the Griess method modified by Bendschneider–Robinson (Metody gidrokhimicheskikh issledovani, 1988). Chl concentration in water samples, considering pheophytin content, was determined by the spectrophotometry. Water samples of about 1.5 L were preliminarily filtered through “Vladipor MFAS-OS-3” membrane filters, 35 mm in diameter, with a pore diameter of 0.8 μm . Then, the filters were dried, dissolved in 5 mL of 90 % acetone, and placed in a refrigerator. A day later, on a UV-3600 (Shimadzu) spectrophotometer, the absorbance of the extract was determined. Prior to pheophytin measuring, the extract was acidified with 2–3 drops of the prepared solution of hydrochloric acid in acetone. The concentrations were calculated using the formulas by Jeffrey and Humphrey (1975) and by Lorenzen (1967).

The thickness of the photic layer (hereinafter PhL) at each station was determined based on the data of a LI-COR QSP-2300L underwater PAR sensor. When probing the water column, vertical PAR profiles were obtained. The lower PhL boundary was taken as the depth of occurrence of 1 % PAR relative to the sensor readings in the surface water layer (1.5–2 m) (Ryther, 1956). For the dark time, the PhL thickness was determined from its dependence of the chlorophyll fluorescence maximum depth (Fig. 2). When having several extrema on the vertical profiles of chlorophyll, the depth of occurrence was used, which corresponded to the maximum of turbidity values. To calculate the PP, chlorophyll fluorescence data obtained during probing were corrected separately for each station (based on laboratory measurements of Chl by the spectrophotometry). The general trend of fluorescence vs. chlorophyll concentration is given in Fig. 3. The graph shows chlorophyll fluorescence measured by a Seapoint Chlorophyll Fluorometer at the depth of water sampling at the time of bathometer closure.

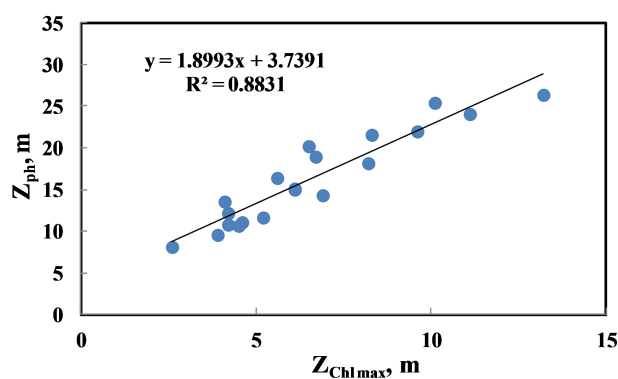


Fig. 2. Dependence of the photic layer depth, Z_{ph} , on chlorophyll maximum depth, $Z_{ChL_{max}}$, during the study on the northeastern Sakhalin Island shelf

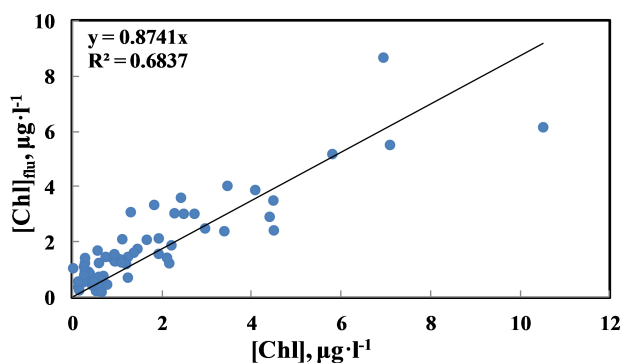


Fig. 3. Dependence of chlorophyll *a* concentration measured by a Seapoint Chlorophyll Fluorometer, $[Chl]_{flu}$, on the data of its laboratory measurements, $[Chl]$

To measure the assimilation number for phytoplankton (hereinafter A_n), water was sampled into 1.7-L bottles; to their necks, ARO1-USB Rinko optical oxygen sensors (JFE Advantech Co., Ltd.) were attached (their technical characteristics are given in Table 1). Using sensors hung overboard to a sampling depth (2 m), *in situ* for 2 h 40 min, oxygen was continuously recorded in the light and dark bottles with an interval of 1 min during a complete stoppage of the RV. This allowed to register temporal variability of oxygen content during incubation and eliminate the random error associated with the measurement of oxygen content in the bottles. At the same time, to determine A_n , linear approximation was applied to the entire data series; initial and final values of DO from the approximation equation were used for the initial and final moments of sample exposure. A_n was measured once (the spot is shown in Fig. 1).

Table 1. Technical characteristics of ARO1-USB Rinko dissolved oxygen sensors

Parameter	Dissolved oxygen	Temperature
Principle	Phosphorescence	Thermistor
Range	Air saturation 0 to 200 %	-3...+45 °C
Resolution	0.01–0.04 %	0.001 °C
Accuracy	Non-linearity ± 2 % of full scale (at 1 atm, +25 °C)	± 0.02 °C (0 to +35 °C)

Since the investigation was carried out within the framework of a complex research cruise, it was impossible to measure A_n at each station. The obtained A_n value was used to calculate the PP for the entire study area. Previously, a similar assumption was made by Yu. Sorokin and P. Sorokin (1999) when studying the PP of the Sea of Okhotsk. When carrying out the measurements, the slope of the time dependence of ΔO_2 did not change; thereby, the A_n value during the measurements was assumed to be constant in the daytime. The assimilation number was calculated according to the formula:

$$A_n = \frac{dO_2}{[Chl] \cdot PQ \cdot t}, \quad (1)$$

where $dO_2 = (O_{lf} - O_{df}) - (O_{l0} - O_{d0})$ is the difference between the final and initial differences in the readings of the sensors in the light and dark bottles, $\text{mg}\cdot\text{L}^{-1}$;

O_{l0} and O_{lf} are initial and final concentrations of oxygen in the light bottle, $\text{mg}\cdot\text{L}^{-1}$;

O_{d0} and O_{df} are initial and final concentrations of oxygen in the dark bottle, $\text{mg}\cdot\text{L}^{-1}$;

$[Chl]$ is chlorophyll *a* concentration, $\mu\text{g}\cdot\text{L}^{-1}$;

PQ is photosynthetic coefficient;

t is exposure time, h.

PQ was taken equal to 1.42. This value corresponds to mesotrophic waters with the prevalence of diatoms (Laws, 1991 ; Smith et al., 2012), and it is characteristic of the study area (Orlova et al., 2004 ; Shevchenko & Ponomareva, 2013).

During the complex work on the northeastern Sakhalin Island shelf on the 71st cruise of the RV “Professor Gagarinsky”, water was also sampled for determining the species composition of phytoplankton (Tishchenko et al., 2018). At the time of the study, diatoms accounted for more than 90 % of the total phytoplankton abundance (personal communication of Yu. Fedorets).

Based on the PhL thickness data and concentrations of Chl and An, phytoplankton primary production in the photic layer was determined. For the calculations, the representation of the photosynthetic light-response curve in the modified model of the non-rectangular hyperbola was used (Tishchenko et al., 2017, 2019 ; Zvalinsky, 2008 ; Zvalinskii et al., 2006) which is largely similar to the Vertically Generalized Production Model (VGPM) (Behrenfeld & Falkowski, 1997). Below, there is the derivation of the equation for calculating the integral PP in the PhL taken from (Tishchenko et al., 2019).

The formula for calculating primary production for the depth Z within the photic layer is as follows:

$$P = P^m \frac{1 + I_z/I_k}{2\gamma} \left\{ 1 - \sqrt{1 - \frac{4\gamma I_z/I_k}{(1 + I_z/I_k)^2}} \right\}, \quad (2)$$

where P^m is the rate of photosynthesis under light saturation, $\text{mg C}\cdot\text{m}^{-2}\cdot\text{day}^{-2}$;

I_z is solar radiation at depth Z, $\mu\text{mol}\cdot\text{m}^{-2}\cdot\text{day}^{-1}$;

I_k is the light constant corresponding to the light intensity at which the light-response curve goes to saturation (Talling, 1957), and it is equal to 10 % of PAR incident on water surface I_0 , $\mu\text{mol}\cdot\text{m}^{-2}\cdot\text{day}^{-1}$;

γ is the non-rectangular hyperbola parameter equal to 0.95 for real light-response curves for seaweed (Zvalinsky, 2008).

Within the photic layer (Z_{ph}), light intensity decreases exponentially with depth (Behrenfeld & Falkowski, 1997 ; Gordon & McCluney, 1975):

$$I_z = I_0 \cdot \exp(-k_d \cdot Z), \quad (3)$$

where k_d is the coefficient of diffuse attenuation of light;

Z is depth, m.

Taking into account that at the lower PhL boundary (*i. e.*, at a compensation depth Z_c) the light intensity $I_c \approx 1$ % PAR (Ryther, 1956) and the fact that $I_k = 0.1I_0$, it was obtain:

$$k_d = \frac{\ln(I_0/I_c)}{Z_c} = \frac{\ln(I_0/0.01I_0)}{Z_c} = 4.6/Z_c, \quad (4)$$

$$I_z/I_k = \frac{I_0 \exp(-k_d Z)}{0.1I_0} = 10 \exp(-4.6Z/Z_c).$$

When numerically integrating equation (2) from the surface horizon, corresponding to light saturation, to Z_c and considering equation (4), a coefficient of 0.66 is obtained which does not depend on the PhL thickness when the site depth is greater than the PhL depth. In this case, the equation for calculating the integral PP takes the following form:

$$P = 0.66 \cdot An \cdot C_{ch} \cdot T_d, \quad (5)$$

where An is the assimilation number for phytoplankton in the subsurface layer, $\text{mg C}\cdot(\text{mg Chl}\cdot\text{h})^{-1}$;

C_{ch} is chlorophyll *a* content in the photosynthesis layer (Z_{ph}), $\text{mg}\cdot\text{m}^{-2}$;

T_d is the length of the day, h.

Chl content in the photosynthesis layer can be obtained by numerical integration of vertical chlorophyll profiles measured by probing equipment:

$$C_{ch} = \sum_i [Chl]_{Z_i}, \quad (6)$$

where

$$[Chl]_{Z_i} = (Z_{i+1} - Z_i) \frac{(Chl_{Z_i} + Chl_{Z_{i+1}})}{2}. \quad (7)$$

An integration step of 10 cm was used to obtain C_{ch} . The coefficient in equation (5) is close in value to that applied in VGPM (Behrenfeld & Falkowski, 1997) which is equal to 0.66125.

The main difference between the model used in the article and the VGPM is that photoinhibition is not directly taken into account here. However, it is taken into account indirectly when measuring A_n since the exposure time for the light and dark bottles is quite long. The second distinction is the description of the light-response curve by the non-rectangular hyperbola. The light-response curve comes to a state of saturation at a value equal to 10 % of PAR incident on surface. With this value, integration of equation (2) leads to the fact that the value of the coefficient in equation (5) is 0.66. The proposed model of photosynthesis showed good agreement with the modified model of the rectangular hyperbola which is capable of describing the photoinhibition of the process by the non-rectangular hyperbola, as well as with field data on CO_2 gas exchange in the leaves of land plants (Korsakova et al., 2018).

RESULTS AND DISCUSSION

Hydrological conditions, nutrients, and chlorophyll *a*. Hydrological conditions on the northeastern slope of Sakhalin in July are formed mainly by the Amur River runoff, which at that time goes around the northern tip of the island, passes along its northeastern coast southward, and forms an area of warm desalinated waters (Rutenko & Sosnin, 2014) (Figs 4, 5). Moreover, it causes a blast phytoplankton bloom (Prants et al., 2017; Tskhay et al., 2015). In some years in autumn, with the maximum Amur River runoff, desalinated waters can pass along the eastern coast southward and reach the Aniva Bay (Tskhay et al., 2015). In this case, the distribution area of these waters is limited by the traverse of the southern boundary of the Piltun Bay. There is a hypothesis that two relatively stable eddy formations may exist in this area of the shelf, and those limit further penetration of desalinated waters southward (Rutenko & Sosnin, 2014).

During our studies, desalinated warm waters of the Amur River (+13 °C, practical salinity (PS) 19) shifted southward along the Sakhalin Island shelf. Opposite the Piltun Bay, those collided with a core of cold salty waters (+1 °C, PS 32) and formed a hydrological front (Figs 4a, 5a). Near-bottom waters were characterized by a uniform decrease in temperature and an increase in salinity with depth (from +8 °C and PS 26 to –1.5 °C and PS 33). In the northern area under study, cold salty waters (+1 °C, PS 32.5) upwelled to the shelf which limited the distribution area of warm desalinated waters to depths of down to 20 m (Fig. 6b, d). In the surface layer, the area of warm desalinated waters was characterized by low content of nitrates and phosphates (Figs 7a, 8a) – no more than 1 and 0.2 $\mu\text{mol}\cdot\text{L}^{-1}$, respectively. In the core of cold salty waters, concentration of nutrients rose significantly: nitrates, up to 11 $\mu\text{mol}\cdot\text{L}^{-1}$; phosphates, up to 1.4 $\mu\text{mol}\cdot\text{L}^{-1}$. With increasing depth, the content of nutrients in water rose: nitrates, up to 18 $\mu\text{mol}\cdot\text{L}^{-1}$; phosphates, up to 1.6 $\mu\text{mol}\cdot\text{L}^{-1}$ (Figs 7b, 8b). Desalinated waters were characterized by an increased content of Chl – up to 12.9 $\mu\text{g}\cdot\text{L}^{-1}$ (Fig. 9a). In the near-bottom water layer,

Chl content varied within $0.1\text{--}10.5\ \mu\text{g}\cdot\text{L}^{-1}$ (Fig. 9b). The highest concentrations in the near-bottom layer were observed at the nearest station, opposite the Piltun Bay. In the core of cold salty waters, concentrations were about $2\ \mu\text{g}\cdot\text{L}^{-1}$; in the near-bottom layer, content decreased to $1\ \mu\text{g}\cdot\text{L}^{-1}$ in the northern area under study and remained at the level of $2\ \mu\text{g}\cdot\text{L}^{-1}$ in its southern area (Fig. 9b).

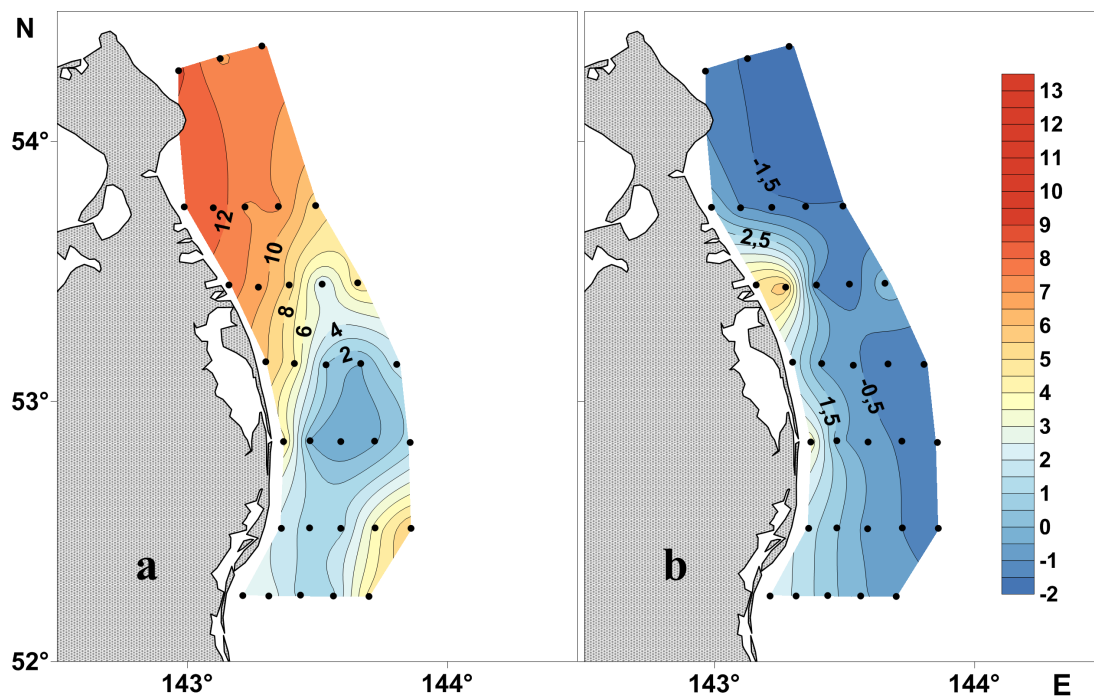


Fig. 4. Spatial distribution of water temperature, °C, on the northeastern Sakhalin Island shelf: a, surface horizon; b, near-bottom horizon (71st cruise of the RV “Professor Gagarinsky”, 7–9 July, 2016)

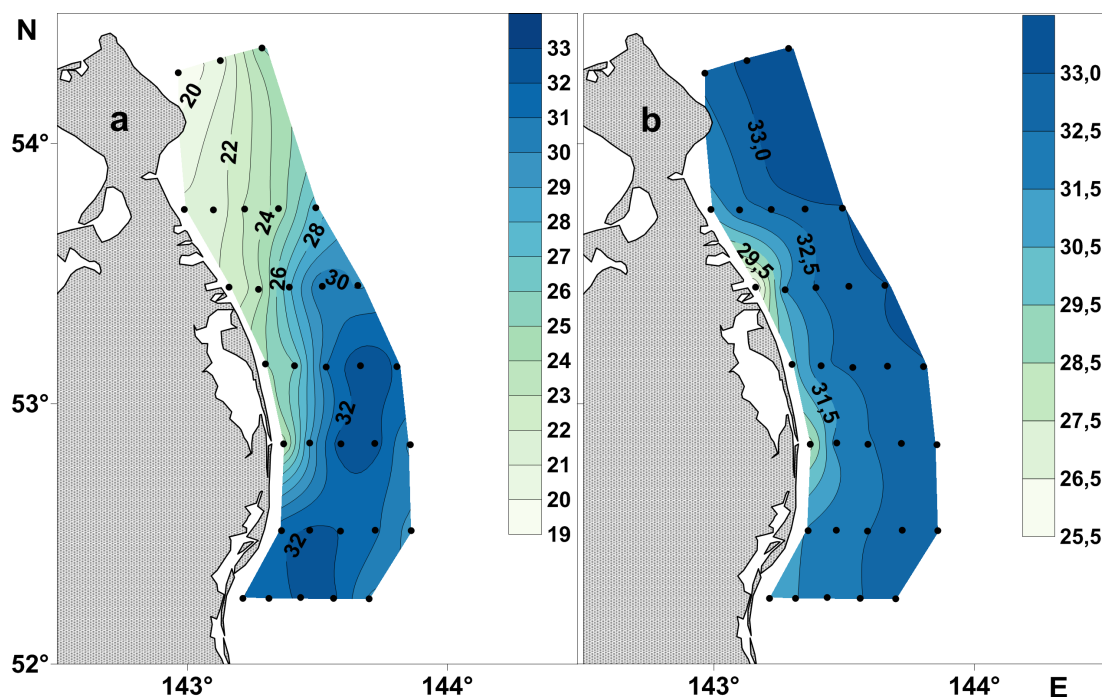


Fig. 5. Spatial distribution of practical salinity on the northeastern Sakhalin Island shelf: a, surface horizon; b, near-bottom horizon (71st cruise of the RV “Professor Gagarinsky”, 7–9 July, 2016)

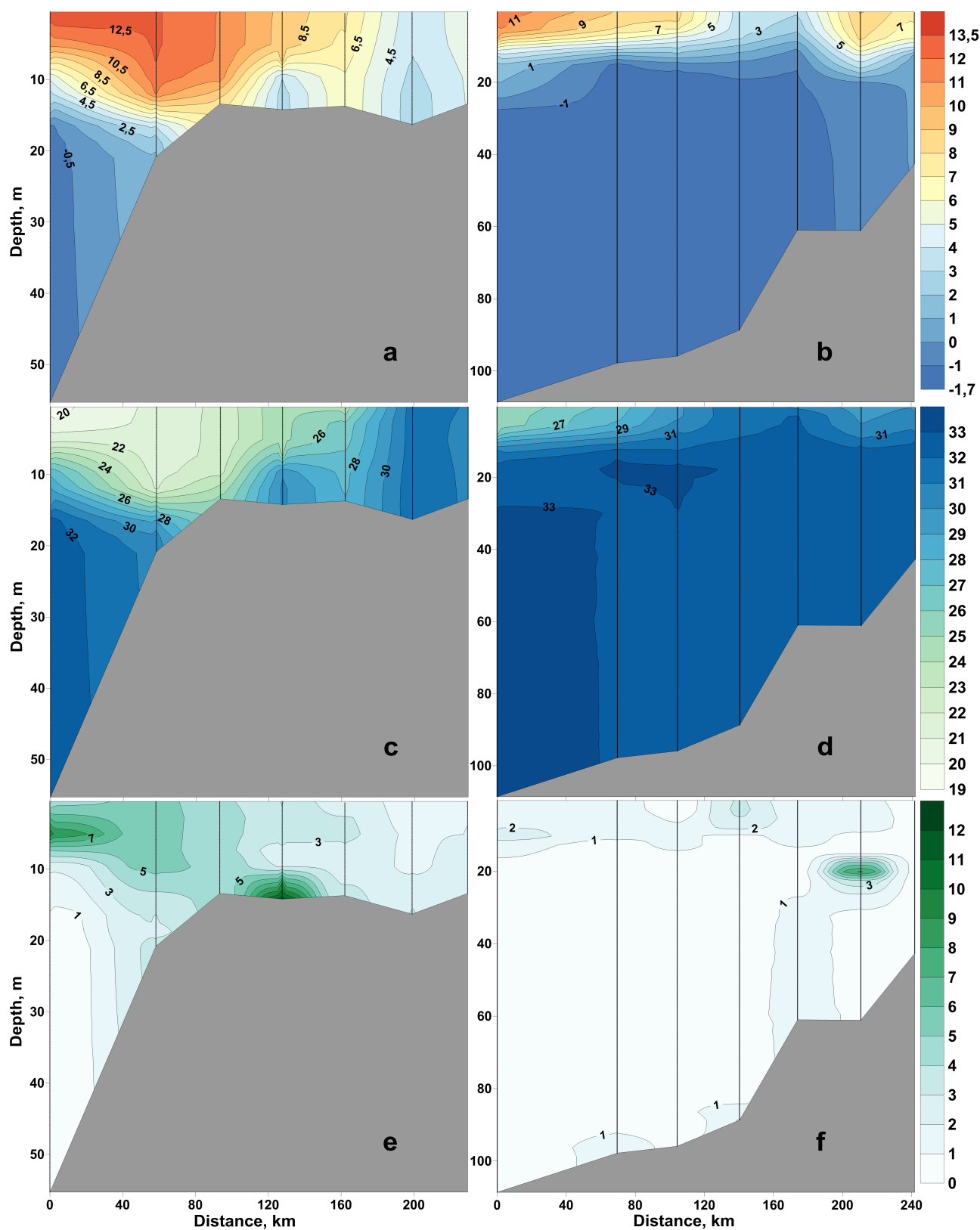


Fig. 6. Depth distribution of temperature, °C (a, b), practical salinity (c, d), and chlorophyll fluorescence, $\mu\text{g}\cdot\text{L}^{-1}$ (e, f), on meridional sections along the northeastern Sakhalin Island shelf through the coastal stations (a, c, e) and the deep-sea stations (b, d, f) (71st cruise of the RV “Professor Gagarinsky”, 7–9 July, 2016). North is on the left

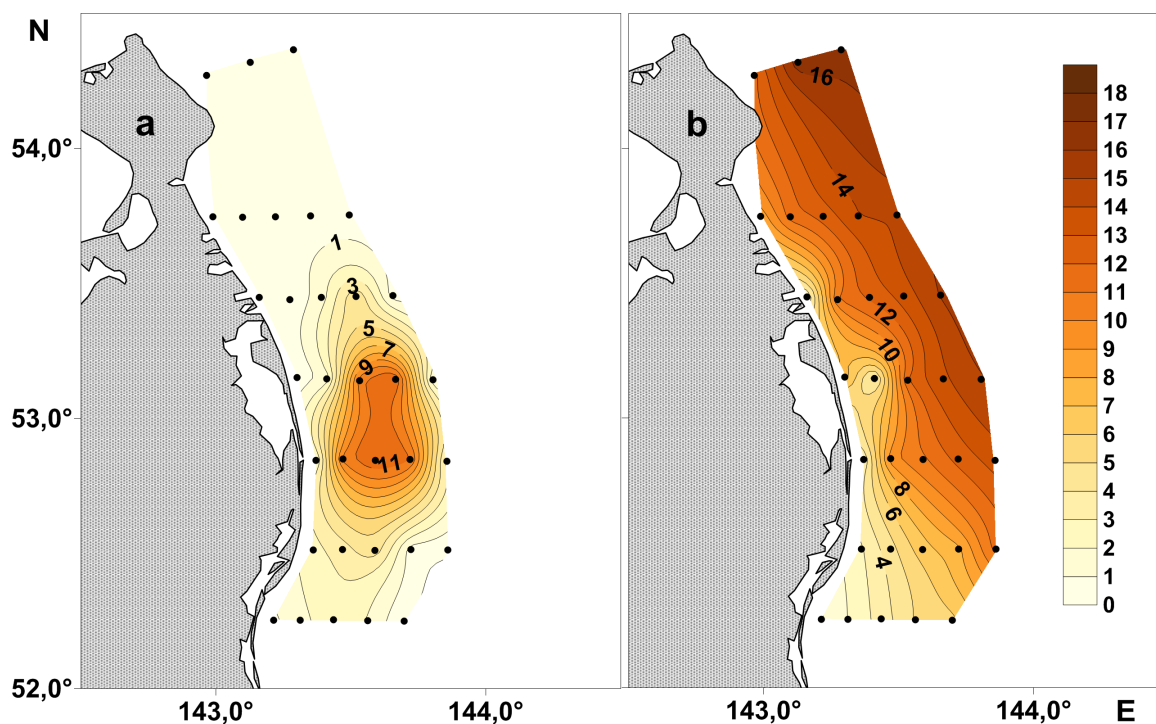


Fig. 7. Spatial distribution of nitrates, $\mu\text{mol}\cdot\text{L}^{-1}$, on the northeastern Sakhalin Island shelf: a, surface horizon; b, near-bottom horizon (71st cruise of the RV “Professor Gagarinsky”, 7–9 July, 2016)

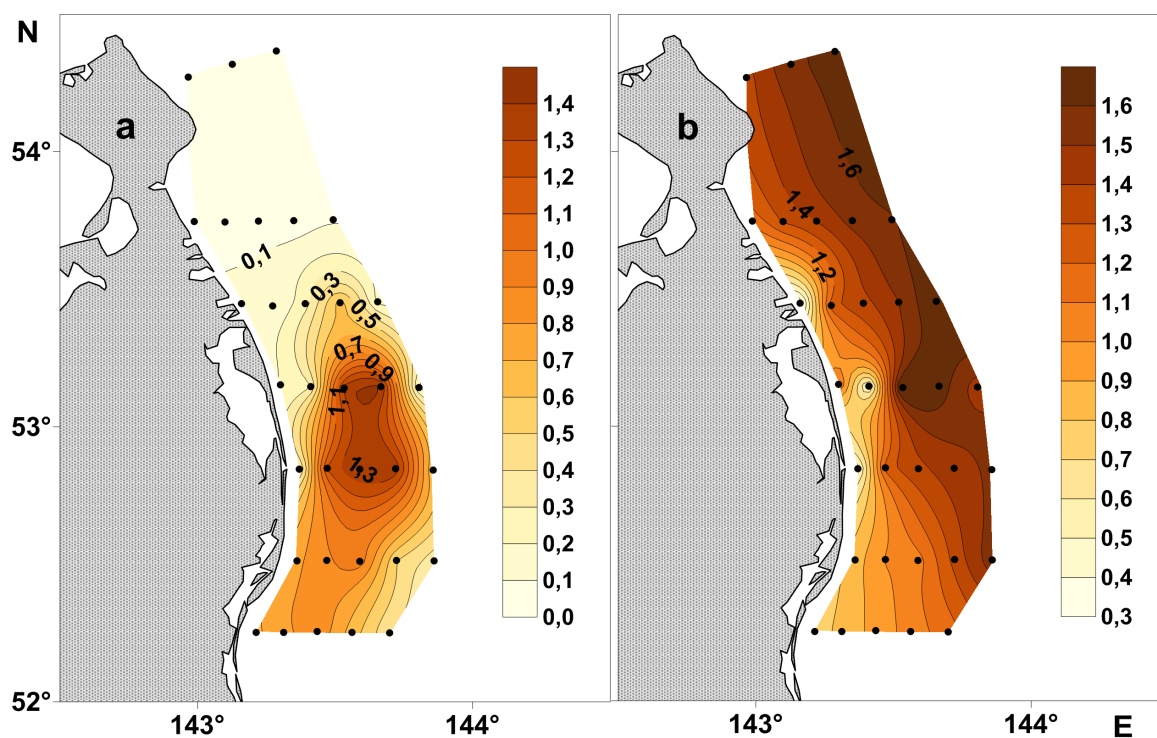


Fig. 8. Spatial distribution of phosphates, $\mu\text{mol}\cdot\text{L}^{-1}$, on the northeastern Sakhalin Island shelf: a, surface horizon; b, near-bottom horizon (71st cruise of the RV “Professor Gagarinsky”, 7–9 July, 2016)

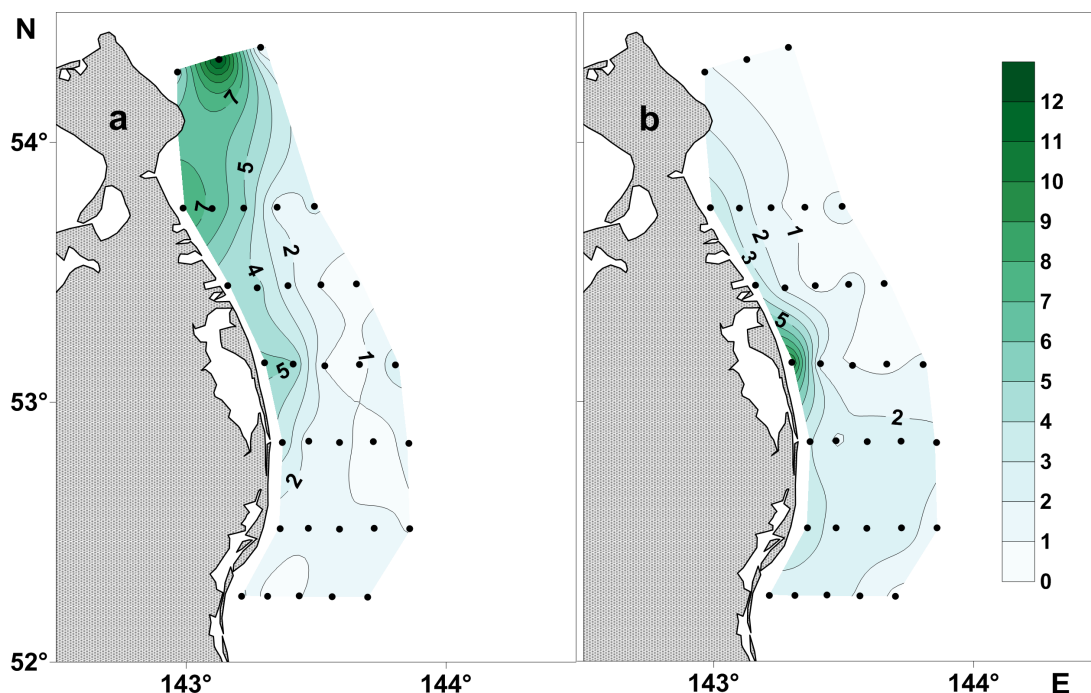


Fig. 9. Spatial distribution of chlorophyll *a*, $\mu\text{g}\cdot\text{L}^{-1}$, on the northeastern Sakhalin Island shelf: a, surface horizon; b, near-bottom horizon (71st cruise of the RV “Professor Gagarinsky”, 7–9 July, 2016)

The nature of spatial distributions of temperature and salinity in the surface layer indicates the penetration of cold salty waters there due to anticyclonic circulation which forms a hydrological front near the Piltun Bay (Figs 4a, 5a). The fact that the penetration of these waters was not a direct consequence of upwelling can be concluded from spatial distributions of temperature and salinity in the near-bottom water layer (Figs 4b, 5b). Moreover, it can be seen on hydrological sections (Fig. 6a–d): in spatial distribution of temperature and salinity in the southern area under study, no northward penetration of cold salty bottom waters was registered. Spatial changes in temperature and salinity were the most pronounced in the surface layer. Apparently, the mass of cold salty waters preventing the penetration of desalinated waters from the north initially rose to the surface from the lower horizons in the southeastern Sakhalin Island shelf and then shifted northward under the effect of an anticyclonic eddy.

The rise of waters from deeper horizons to the surface due to coastal upwelling (Prants et al., 2017) or the effect of an anticyclonic eddy (Rutenko & Sosnin, 2014) and their subsequent shift northward supplied large amounts of nitrogen and phosphorus into the surface layer. Specifically, their concentrations were comparable to the values corresponding to near-bottom water layers (Figs 7, 8). The desalinated water area was characterized by relatively low content of inorganic substances of nitrogen and phosphorus (Figs 7a, 8a). Presumably, this resulted from an increased photosynthetic activity of phytoplankton in the desalinated water area. Chl spatial distribution in the surface layer indirectly confirms this assumption (Fig. 9): high Chl concentrations were recorded in waters with low content of nutrients. In the northern area of the bay which is under maximum effect of the Amur River, Chl content in water reached $12.9 \mu\text{g}\cdot\text{L}^{-1}$. In the area of the hydrological front, it decreased to $2 \mu\text{g}\cdot\text{L}^{-1}$. Interestingly, in the area of cold salty waters, where the content of nutrients is maximum, Chl concentrations were about $2 \mu\text{g}\cdot\text{L}^{-1}$ (Fig. 8a). Based on this, it can be assumed that the photosynthetic activity of phytoplankton is low in the core of cold salty waters. Apparently, intensive development of phytoplankton in these waters could result from their heating.

High values of chlorophyll fluorescence in the near-bottom water layer recorded at one of the coastal stations, opposite the Piltun Bay, have to be noted as well. Probably, sedimentation of organic matter to the bottom occurs here; this can also be assumed from the position of the isolines in the vertical fluorescence section (Fig. 6e).

Measurements of the assimilation number. During the entire exposure time, an increase in oxygen content in the light bottle was observed (Fig. 10a). The increase was non-linear. Specifically, during the first hour of exposure, the rate of O₂ increase was 0.22 mg·L⁻¹·h⁻¹; then, it slowed down to 0.05 mg·L⁻¹·h⁻¹. In the dark bottle, during the first hour of exposure, O₂ content increased as well (the rate was of 0.15 mg·L⁻¹·h⁻¹). Then, oxygen concentration began to decrease (the rate was of -0.11 mg·L⁻¹·h⁻¹).

Interestingly, the difference in readings between the light and dark bottles steadily increased with time. So, changes in the rate of decrease/increase in the level of oxygen in the samples obeyed the same laws and were not an experimental error. During the exposure, water temperature in the samples rose by 1.5 °C (Fig. 10b), and the increase was non-linear. The change in the difference in oxygen readings between the light and dark bottles occurred according to a linear law (Fig. 10c). Also, the linear increase in ΔO₂ values was not affected by a low temperature difference in the samples (Fig. 10b, c) which was noted earlier (Tishchenko et al., 2017). The maximum temperature difference between the light and dark bottles was of 0.508 °C, and this corresponded to the largest single deviations of ΔO₂ from the linear approximation reaching 0.038 mg·L⁻¹ at ΔO₂ = 0.369 mg·L⁻¹. The total exposure time was 2 h 40 min. Only the initial and final values of the time dependence of ΔO₂ were used to calculate An, but the entire series of measurements is given in the article to prove the quality of the data obtained. Chlorophyll content in water before exposure was 3.85 μg·L⁻¹. According to the results of the experiment, the obtained value of the assimilation number was 9.66 mg C·(mg Chl·h)⁻¹. Such a high rate of carbon assimilation may be due to increased content of iron introduced by the Amur River waters (Nishioka et al., 2014 ; Shulkin & Zhang, 2014). The shadow growth of oxygen recorded during the experiment is a periodically observed phenomenon (Cherbadgy & Propp, 2008 ; Ettwig et al., 2012 ; Pamatmat, 1997 ; Pospíšil, 2007). There is no single and generally accepted explanation. Apparently, the shadow growth of O₂ results from the decomposition of hydrogen peroxide (Cherbadgy & Propp, 2008) and production of bacteria (Ettwig et al., 2012).

Phytoplankton primary production. Phytoplankton PP values varied from 1.57 to 11.17 g C·m⁻²·day⁻¹. The nature of spatial variability of the PP coincided with that of Chl spatial distribution in the surface water layer: the highest PP values were confined to the northern area under study which is under maximum effect of the Amur River (Figs 9, 11). As shifting southward, the PP decreased and reached its minimum values in the southeastern area under study and in the area of cold salty waters. Obviously, this nature of the PP distribution corresponds to the period of maximum effect of the Amur River runoff since in August–September the value of phytoplankton production on the northeastern Sakhalin Island shelf is about 0.7–0.8 g C·m⁻²·day⁻¹. Abeam the southern boundary of the Chayvo Bay, where the effect of the Amur River runoff is low, the obtained PP values correspond to the values typical for August–September (Isada et al., 2009). Thus, the phytoplankton bloom on the northeastern Sakhalin Island shelf is strongly dependent on the runoff volume of the Amur River, under the effect of which Chl content in the bloom area can vary fourfold (Tskhay et al., 2015).

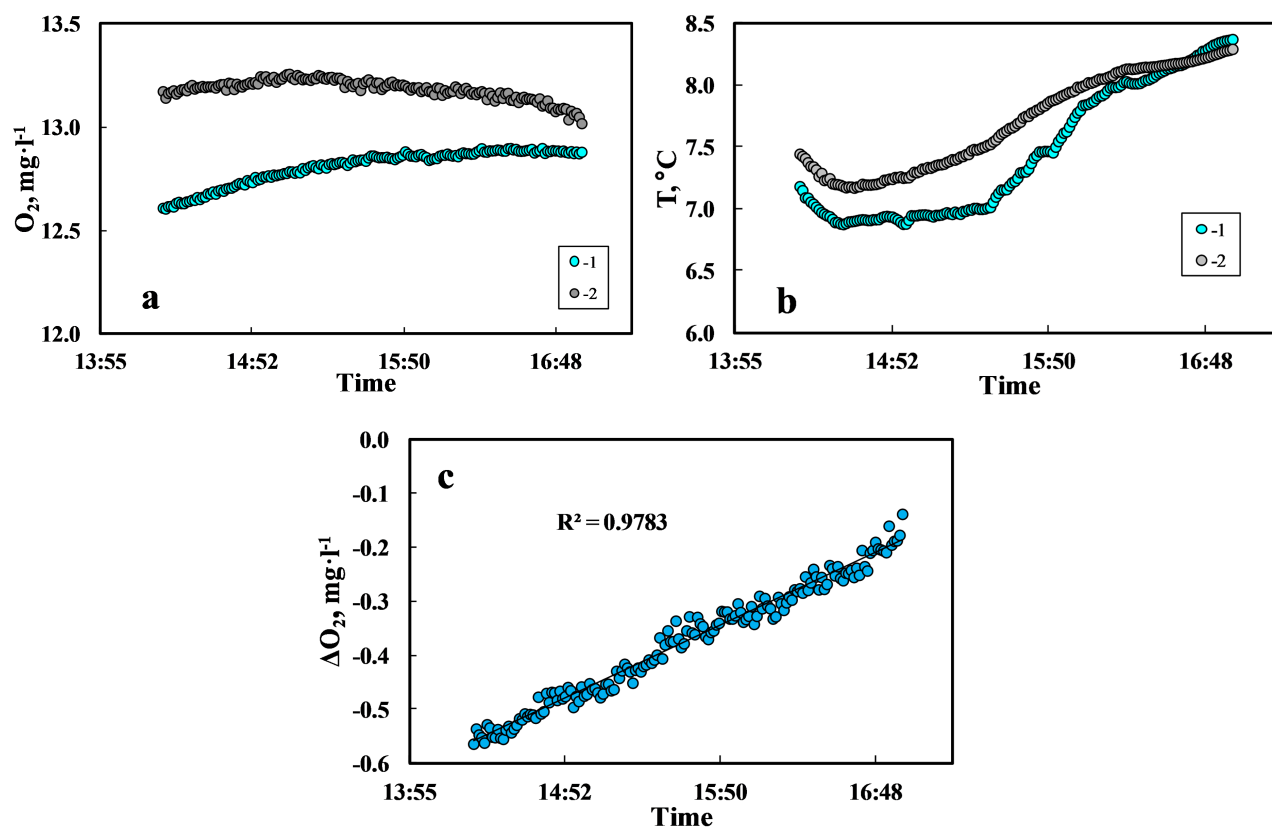


Fig. 10. Time variability of oxygen concentration (a), water temperature (b), and difference in readings for dark and light bottles (c) for ARO1-USB Rinko dissolved oxygen sensors on the northeastern Sakhalin Island shelf on 8 July, 2016: ● denotes a light bottle; ● denotes a dark bottle. The abscissa shows the local time

Apparently, the high production on the northeastern slope of the Sakhalin is due to the Amur River runoff since it is a source of iron (Nishioka et al., 2014 ; Shulkin & Zhang, 2014) actively involved in phytoplankton fertilization on the eastern island shelf (Kanna et al., 2018 ; Yoshimura et al., 2010). For the PP, iron is the key nutrient: its absence leads to formation of water areas with high nitrogen and phosphorus concentrations and low production in the photic layer in the open ocean (Martin & Fitzwater, 1988). The Amur River plays a significant role in the PP formation not only on the northeastern slope of Sakhalin Island studied in this work but in a large area of the Sea of Okhotsk and even in the Kuril Islands area (Nishioka et al., 2014). Our results emphasize the importance of the Amur River runoff in the PP formation.

Assessment of the feeding area for gray whales. The coastal zone from the Urkt Bay to the middle Chayvo Bay with depths down to 20 m, which is a feeding area for gray whales, covers about 600 km^2 (Bröker et al., 2020). With a mean PP value of $6.5 \text{ g C} \cdot \text{m}^{-2} \cdot \text{day}^{-1}$, the total phytoplankton production there will reach $3,900 \text{ t C} \cdot \text{day}^{-1}$. Considering that carbon content is 10 % of the phytoplankton biomass, it corresponds to $39,000 \text{ t} \cdot \text{day}^{-1}$ wet weight of phytoplankton (Menden-Deuer & Lessard, 2000). Assuming that the biomass of the secondary link in the food chain averages 0.1 of the biomass of the primary link (Odum, 1971), the value of zooplankton/zoobenthos production in the feeding area of gray whales will be $3,900 \text{ t} \cdot \text{day}^{-1}$ wet weight. The biomass required for daily feeding of gray whale averages $409 \text{ kg} \cdot \text{day}^{-1}$ (Bröker et al., 2020). Based on general considerations, the coastal zone from the Urkt Bay to the Chayvo Bay can serve as a feeding area for 9,500 whales. This value is consistent with historical

data: previously, the Okhotsk–Korean population of gray whales was estimated at 1,500–10,000 individuals (Berzin, 1974 ; Yablokov & Bogoslovskaya, 1984). In 2014–2015, the Okhotsk–Korean population was of 172–186 individuals (Bröker et al., 2020 ; Cooke et al., 2015). With a population of ~ 180 individuals, 736 t·day⁻¹ wet weight of phytoplankton is required to form a food supply; it is 1.9 % of the total productivity of the studied water area.

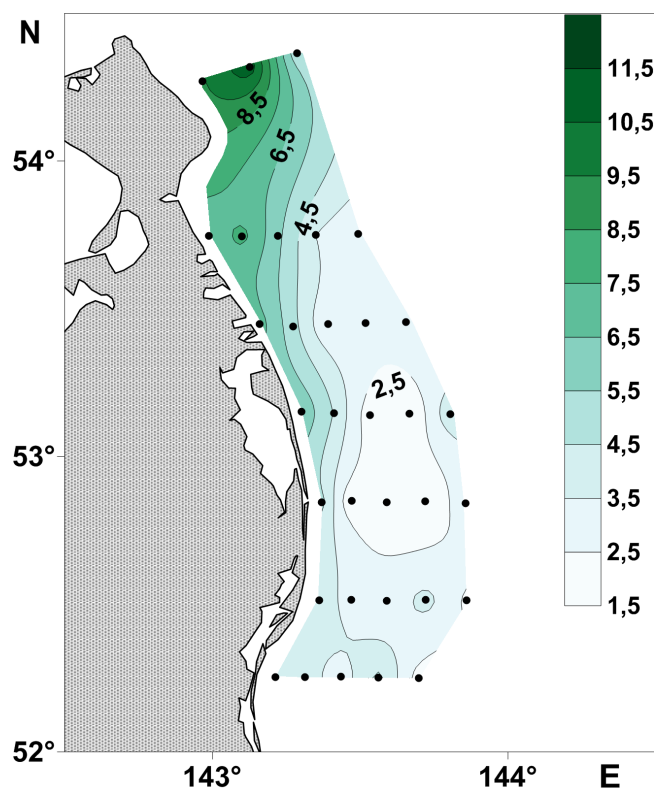


Fig. 11. Spatial distribution of phytoplankton primary production, g C·m⁻²·day⁻¹, on the northeastern Sakhalin Island shelf (7–9 July, 2016)

Conclusion. As found during the study, the formation of phytoplankton primary production occurred most intensively in waters most affected by the Amur River runoff and coastal runoff. The effect of these waters extended up to the traverse of the southern boundary of the Piltun Bay; there, it was limited by cold salty water which had risen to the south of the study area due to the eddy structure from deeper horizons. The obtained high value of the assimilation number of phytoplankton characterizes the high rate of photosynthesis there. Primary production in the photic layer in the area of maximum effect of the Amur River reached 11.17 g C·m⁻²·day⁻¹. The total phytoplankton primary production in the depth range down to 20 m, which is necessary for a food supply formation for gray whales, with a population of ~ 180 individuals, is 736 t·day⁻¹ of phytoplankton wet weight, or 1.9 % of the total productivity of the studied water area.

This work was financially supported by the Russian Foundation for Basic Research (grant No. 21-55-53015) and programs of fundamental research (topics No. 121021500052-9 and 121021700346-7).

Acknowledgement. The author is grateful to the captain of the RV “Professor Gagarinsky” Eduard Gavailer, the crew members, and the scientific staff for comprehensive assistance in the cruise, as well as to Yuliya Fedorets for providing information on the species composition of phytoplankton in the studied area during the expedition work.

REFERENCES

1. Berzin A. A. Aktual'nye problemy izucheniya kitoobraznykh (na primere kitoobraznykh Tikhogo okeana). In: *Zoologiya bespozvonochnykh*. Moscow : VINITI, 1974, pp. 159–189. (Itogi nauki i tekhniki ; vol. 6). (in Russ.)
2. Zvalinsky V. I. Quantitative description of marine ecosystems. I. General approach. *Izvestiya TINRO*, 2008, vol. 152, pp. 132–153. (in Russ.)
3. Zvalinskii V. I., Lobanov V. B., Zakharkov S. P., Tishchenko P. Ya. Chlorophyll, delayed fluorescence, and primary production in the north-western part of the Sea of Japan. *Oceanology*, 2006, vol. 46, iss. 1, pp. 27–37. (in Russ.). <https://doi.org/10.1134/S0001437006010048>
4. Korsakova S. P., Ilnitsky O. A., Plugar Yu. V. Comparison of photosynthetic light-response curves models by the example of evergreen plant species. *Nauka Yuga Rossii [Science in the South Russia]*, 2018, vol. 14, no. 3, pp. 88–100. (in Russ.). <https://doi.org/10.7868/S25000640180310>
5. *Metody gidrokhimicheskikh issledovaniy osnovnykh biogennykh elementov*. Moscow : VNIRO, 1988, 120 p. (in Russ.)
6. Orlova T. Yu., Selina M. S., Stonik I. V. Species composition of planktonic microalgae of coastal waters of Sakhalin Island, Sea of Okhotsk. *Biologiya morya*, 2004, vol. 30, no. 2, pp. 96–104. (in Russ.)
7. Rutenko A. N., Sosnin V. A. Hydrodynamic processes on the Sakhalin shelf in the coastal Piltun area of the grey whale feeding and their correlation with atmospheric circulation. *Meteorologiya i gidrologiya*, 2014, no. 5, pp. 74–93. (in Russ.). <https://doi.org/10.3103/S1068373914050070>
8. Tishchenko P. P., Tishchenko P. Ya., Zvalinsky V. I., Semkin P. Yu. The primary production of Amursky Bay (Sea of Japan) in the summer of 2008. *Biologiya morya*, 2017, vol. 43, no. 3, pp. 195–202. (in Russ.). <https://doi.org/10.1134/S1063074017030117>
9. Tishchenko P. Ya., Lobanov V. B., Shulkin V. M., Melnikov V. V., Tsoi I. B., Semkin P. Yu., Tishchenko P. P., Bannov V. A., Belous O. V., Vasileva L. E., Elovskaya O. A., Sagalaev S. G., Fedorets Yu. V. Comprehensive research of the coastal water area of the Sea of Japan and Sea of Okhotsk under the influence of river runoff (Cruise 71 of the RV “Professor Gagarinskii”). *Oceanology*, 2018, vol. 58, iss. 2, pp. 340–342. (in Russ.). <https://doi.org/10.1134/S0001437018010150>
10. Tishchenko P. P., Tishchenko P. Ya., Elovskaya O. A., Zvalinsky V. I., Fedorets Yu. V. Conditions for primary production of phytoplankton in the Vostok Bay (Japan Sea) in spring 2016. *Izvestiya TINRO*, 2019, vol. 198, pp. 164–185. (in Russ.). <https://doi.org/10.26428/1606-9919-2019-198-164-185>
11. Tskhay Zh. R., Shevchenko G. V., Chastikov V. N. Anomal'noe vliyanie stoka reki Amur na gidrologicheskie usloviya shel'fa o. Sakhalin v period pavodka 2013 goda. In: *Geodynamic Processes and Natural Hazards. Lessons of Neftegorsk : vserossiiskaya nauchnaya konferentsiya s mezhdunarodnym uchastiem*, 26–30 May, 2015, Yuzhno-Sakhalinsk, Russia : sbornik materialov : [in 2 vols]. Vladivostok : Dal'nauka, 2015, vol. 1, pp. 386–389. (in Russ.)
12. Cherbady I. I., Propp L. N. Photosynthesis and respiration of a deep-water periphyton community (Macclesfield Bank, South China Sea). *Biologiya morya*, 2008, vol. 34, no. 5, pp. 351–358. (in Russ.). <https://doi.org/10.1134/S1063074008050064>
13. Shevchenko O. G., Ponomareva A. A. Phytoplankton on the north-eastern coast of Sakhalin Island in August–September 2010. *Nauchnye trudy Dal'rybvтуza*, 2013, vol. 29, pp. 31–40. (in Russ.)
14. Behrenfeld M. J., Falkowski P. G. A consumer's guide to phytoplankton primary production models. *Limnology and Oceanography*, 1997, vol. 42, iss. 7, pp. 1479–1491. <https://doi.org/10.4319/lo.1997.42.7.1479>
15. Bröker K. C. A., Gailey G., Tyurneva O. Yu., Yakovlev Yu. M., Sychenko O., Dupont J. M.,

- Vertyankin V. V., Shevtsov E., Drozdov K. A. Site-fidelity and spatial movements of western North Pacific gray whales on their summer range off Sakhalin, Russia. *PLoS ONE*, 2020, vol. 15, iss. 8, art. no. e0236649 (27 p.). <https://doi.org/10.1371/journal.pone.0236649>
16. Cooke J., Weller D., Bradford A., Sychenko O., Burdin A., Lang A. Updated population assessment of the Sakhalin gray whale aggregation based on the Russia–US photoidentification study at Piltun, Sakhalin, 1994–2014. *Western Gray Whale Advisory Panel Doc. WGWAP/16/17* : 16th meeting, Moscow, 22–24 Nov., 2015. [Moscow, 2015], 11 p.
17. Ettwig K. F., Speth D. R., Reimann J., Wu M. L., Jetten M. S., Keltjens J. T. Bacterial oxygen production in the dark. *Frontiers in Microbiology*, 2012, vol. 3, art. no. 273 (8 p.). <https://doi.org/10.3389/fmicb.2012.00273>
18. Gordon H. R., McCluney W. R. Estimation of the depth of sunlight penetration in the sea for remote sensing. *Applied Optics*, 1975, vol. 14, iss. 2, pp. 413–416. <https://doi.org/10.1364/AO.14.000413>
19. Isada T., Suzuki K., Liu H., Nishioka J., Nakatsuka T. Primary productivity and photosynthetic features of phytoplankton in the Sea of Okhotsk during late summer. In: *Proceedings of the Fourth Workshop on the Okhotsk Sea and Adjacent Areas* / M. Kashiwai, G. A. Kantakov (Eds). Sidney, B. C., Canada : PICES, 2009, pp. 72–75. (PICES Scientific Report ; no. 36).
20. Jeffrey S. W., Humphrey G. F. New spectrophotometric equations for determining chlorophylls *a*, *b*, *c*₁ and *c*₂ in higher plants, algae and natural phytoplankton. *Biochimie und Physiologie der Pflanzen*, 1975, vol. 167, iss. 2, pp. 191–194. [https://doi.org/10.1016/S0015-3796\(17\)30778-3](https://doi.org/10.1016/S0015-3796(17)30778-3)
21. Kanna N., Sibano Yu., Toyota T., Nishioka J. Winter iron supply processes fueling spring phytoplankton growth in a subpolar marginal sea, the Sea of Okhotsk: Importance of sea ice and the East Sakhalin Current. *Marine Chemistry*, 2018, vol. 206, pp. 109–120. <https://doi.org/10.1016/j.marchem.2018.08.006>
22. Kasai H., Hirakawa K. Seasonal changes of primary production in the southwestern Okhotsk Sea off Hokkaido, Japan during the ice-free period. *Plankton and Benthos Research*, 2015, vol. 10, iss. 4, pp. 178–186. <https://doi.org/10.3800/pbr.10.178>
23. Laws E. A. Photosynthetic quotients, new production and net community production in the open ocean. *Deep Sea Research Part A. Oceanographic Research Papers*, 1991, vol. 38, iss. 1, pp. 143–167. [https://doi.org/10.1016/0198-0149\(91\)90059-O](https://doi.org/10.1016/0198-0149(91)90059-O)
24. Menden-Deuer S., Lessard E. J. Carbon to volume relationships for dinoflagellates, diatoms, and other protist plankton. *Limnology and Oceanography*, 2000, vol. 45, iss. 3, pp. 569–579. <https://doi.org/10.4319/lo.2000.45.3.0569>
25. Lorenzen C. J. Determination of chlorophyll and pheo-pigments: Spectrophotometric equations. *Limnology and Oceanography*, 1967, vol. 12, iss. 2, pp. 343–346. <https://doi.org/10.4319/lo.1967.12.2.0343>
26. Martin J. H., Fitzwater S. E. Iron deficiency limits phytoplankton growth in the north-east Pacific subarctic. *Nature*, 1988, vol. 331, pp. 341–343. <https://doi.org/10.1038/331341a0>
27. Nishioka J., Nakatsuka T., Ono K., Volkov Yu. N., Scherbinin A., Shiraiwa T. Quantitative evaluation of iron transport processes in the Sea of Okhotsk. *Progress in Oceanography*, 2014, vol. 126, pp. 180–193. <https://doi.org/10.1016/j.pocean.2014.04.011>
28. Odum E. P. *Fundamentals of Ecology*. 3rd edition. Philadelphia, PA : W. B. Saunders Company, 1971, 574 p.
29. Pamatmat M. M. Non-photosynthetic oxygen production and non-respiratory oxygen uptake in the dark: A theory of oxygen dynamics in plankton communities. *Marine Biology*, 1997, vol. 129, pp. 735–746. <https://doi.org/10.1007/s002270050216>
30. Pospíšil P., Šnyrychová I., Nauš J. Dark production of reactive oxygen species in photosystem II membrane particles at elevated temperature: EPR spin-trapping study. *Biochimica et Biophysica Acta (BBA) – Bioenergetics*,

- 2007, vol. 1767, iss. 6, pp. 854–859. <https://doi.org/10.1016/j.bbabi.2007.02.011>
31. Prants S. V., Andreev A. G., Uleysky M. Yu., Budyansky M. V. Mesoscale circulation along the Sakhalin Island eastern coast. *Ocean Dynamics*, 2017, vol. 67, pp. 345–356. <https://doi.org/10.1007/s10236-017-1031-x>
32. Ryther J. H. The measurement of primary production. *Limnology and Oceanography*, 1956, vol. 1, iss. 2, pp. 72–84. <https://doi.org/10.4319/lo.1956.1.2.0072>
33. Smith L. M., Silver C. M., Oviatt C. A. Quantifying variation in water column photosynthetic quotient with changing field conditions in Narragansett Bay, RI, USA. *Journal of Plankton Research*, 2012, vol. 34, iss. 5, pp. 437–442. <https://doi.org/10.1093/plankt/fbs011>
34. Sorokin Yu. I., Sorokin P. Yu. Production in the Sea of Okhotsk. *Journal of Plankton Research*, 1999, vol. 21, iss. 2, pp. 201–230. <https://doi.org/10.1093/plankt/21.2.201>
35. Sorokin Yu. I., Sorokin P. Yu. Microplankton and primary production in the Sea of Okhotsk in summer 1994. *Journal of Plankton Research*, 2002, vol. 24, iss. 5, pp. 453–470. <https://doi.org/10.1093/plankt/24.5.453>
36. Shulkin V., Zhang J. Trace metals in estuaries in the Russian Far East and China: Case studies from the Amur River and the Changjiang. *Science of the Total Environment*, 2014, vol. 499, pp. 196–211. <https://doi.org/10.1016/j.scitotenv.2014.08.015>
37. Shuntov V. P., Ivanov O. A., Dulepova E. P. Biological resources in the Sea of Okhotsk Large Marine Ecosystem: Their status and commercial use. *Deep Sea Research Part II: Topical Studies in Oceanography*, 2019, vol. 163, pp. 33–45. <https://doi.org/10.1016/j.dsr2.2019.01.006>
38. Talling J. F. Photosynthetic characteristics of some freshwater plankton diatoms in relation to underwater radiation. *New Phytologist*, 1957, vol. 56, iss. 1, pp. 29–50. <https://doi.org/10.1111/j.1469-8137.1957.tb07447.x>
39. Yablokov A. V., Bogoslovskaya L. S. 20 – A review of Russian research on the biology and commercial whaling of the gray whale. In: *The Gray Whale: Eschrichtius robustus* / M. L. Jones, S. I. Swartz, S. Leatherwood (Eds). Orlando, FL : Academic Press, 1984, pp. 465–485. <https://doi.org/10.1016/B978-0-08-092372-7.50026-1>
40. Yoshimura T., Nishiona J., Nakatsuka T. Iron nutritional status of the phytoplankton assemblage in the Okhotsk Sea during summer. *Deep Sea Research Part I: Oceanographic Research Papers*, 2010, vol. 57, iss. 11, pp. 1454–1464. <https://doi.org/10.1016/j.dsr.2010.08.003>

ПЕРВИЧНАЯ ПРОДУКЦИЯ ФИТОПЛАНКТОНА НА СЕВЕРО-ВОСТОЧНОМ ШЕЛЬФЕ ОСТРОВА САХАЛИН В ЛЕТНИЙ ПЕРИОД

П. П. Тищенко

Тихоокеанский океанологический институт имени В. И. Ильичёва ДВО РАН,

Владивосток, Российская Федерация

E-mail: eq15@poi.dvo.ru

Восточный шельф острова Сахалин относится к акваториям с высокой биологической продукцией. Его важная отличительная черта — наличие районов нагула для охотско-корейской популяции серых китов. Цель настоящей работы — определить особенности формирования первичной продукции в данном регионе. Для этого в период с 7 по 9 июля 2016 г. были проведены гидрохимические исследования северо-восточного шельфа острова Сахалин. На каждой станции с поверхностного и придонного горизонтов проводили отбор проб воды с последующими измерениями концентраций хлорофилла *a*, нитратов и фосфатов. Также на каждой станции проводили вертикальное зондирование водной толщи с помощью зондов Sea-Bird SBE 19plus V

и Rinko-Profiler, оснащённых датчиками давления, температуры, электропроводности, флуоресценции хлорофилла, растворённого кислорода, мутности и фотосинтетически активной радиации. Датчиками кислорода ARO1-USB Rinko фирмы JFE Advantech Co., Ltd. в условиях *in situ* провели измерения, позволившие рассчитать ассимиляционное число фитопланктона. По результатам исследований определили первичную продукцию фитопланктона в фотическом слое. Для расчёта использовали представление световой кривой в модифицированной модели непрямоугольной гиперболы. Синтез первичной продукции происходил наиболее интенсивно в зоне влияния реки Амур, а значения интегральной первичной продукции в фотическом слое вод изменялись от 1,57 до 11,17 г С·м⁻²·сут⁻¹. Область распространения модифицированных высокопродуктивных вод реки Амур достигала траверза южной границы залива Пильтун, где была ограничена холодными солёными водами, привнесёнными вихревой структурой из глубинных горизонтов. Доля продукции, затрачиваемой на формирование кормовой базы охотско-корейской популяции серых китов, составила 1,9 % от общей продукции рассматриваемой акватории.

Ключевые слова: первичная продукция фитопланктона, река Амур, остров Сахалин, серый кит